IUPAC Task Group on Atmospheric Chemical Kinetic Data Evaluation
Data Sheet MD1; V.A2.1

 The citation for this datasheet is: Crowley, J. N., Ammann, M., Cox, R. A., Hynes, R. G., Jenkin, M. E., Mellouki, A., Rossi, M. J., Troe, J., and Wallington, T. J., Atmos. Chem. Phys., 10, 9059-9223, 2010; IUPAC Task Group on Atmospheric Chemical Kinetic Data Evaluation, http://iupac.pole-ether.fr.

This datasheet last evaluated: June 2016; last change in preferred values: January 2009

O_3 + mineral oxide (dust) surfaces

Experimental data

Parameter	Temp ./K	RH /%	substrate	Reference	Technique/ Comments
γ_0,γ_{ss}					
$\gamma_{ss}^{BET} = (1.4\pm0.35) \times10^{-6}$	295		SiO_2	Il'in et al., 1992	SR-UV (a)
$\gamma_0^{BET} = (8\pm5)\times10^{-5}$ () $\gamma_0^{BET} = (1.8\pm0.7)\times10^{-4}$ $\gamma_0^{BET} = (5\pm3)\times10^{-5}$ $\gamma_0^{BET} = (2.7\pm0.9)\times10^{-5}$ $\gamma_0^{BET} = (6\pm3)\times10^{-5}$ $\gamma_0^{BET} = (4\pm2)\times10^{-6}$	296		α-Al_2O_3 α- Fe_2O_3 SiO_2 China L. Sah. D. Sah. D.	Michel, et al., 2002	Kn-MS (b)
$\gamma_0^{BET} = (1.4\pm0.3) \times10^{-4}$ (25µm) $\gamma_{ss}^{BET} = 7.6 \times 10^{-6}$ (25µm) $\gamma_0^{BET} = (9\pm3)\times10^{-5}$ (1µm) $\gamma_0^{BET} = (2.0\pm0.3)\times10^{-4}$ $\gamma_{ss}^{BET} = 2.2 \times 10^{-5}$ $\gamma_0^{BET} = (6.3\pm0.9)\times10^{-5}$ $\gamma_0^{BET} = (3\pm1)\times10^{-5}$ () $\gamma_0^{BET} = (2.7\pm0.8)\times10^{-5}$ (sand) $\gamma_0^{BET} = (6\pm2)\times10^{-5}$ (ground) $\gamma_{ss}^{BET} = 6 \times 10^{-6}$ (ground) $\gamma_0^{BET} = (2.7\pm0.9)\times10^{-6}$ (<50µm)	295		α-Al_2O_3 α-Al_2O_3 α-Al_2O_3 α-Fe_2O_3 α-Fe_2O_3 SiO_2 kaolinite China L. Sah. D. Sah. D. Sah. D.	Michel, Usher and Grassian, 2003	Kn-MS (c)
$\gamma_0^{pd} = (5.5 \pm3.5)\times10^{-6}$ ($[O_3]=8.4\times10^{12}$ cm^{-3} O_3) $\gamma_0^{pd} = (3.5 \pm3.0)\times10^{-4}$ ($[O_3]=5.4\times10^{10}$ cm^{-3} O_3) $\gamma_{ss}^{pd} = (2.2 \pm1.3)\times10^{-6}$ ($[O_3]=8.4\times10^{12}$ cm^{-3} O_3) $\gamma_{ss}^{pd} = (4.8 \pm2.8)\times10^{-5}$ ($[O_3]=5.4\times10^{10}$ cm^{-3} O_3)	296		Sah. D. Sah. D. Sah. D. Sah. D.	Hanisch and Crowley, 2003	Kn-MS (d)
$\gamma_0^{BET} = 1.0\times10^{-5}$ ($[O_3]=10^{13}$ cm^{-3}) $\gamma_0^{BET} = 1.0\times10^{-6}$ ($[O_3]=10^{14}$ cm^{-3})	298		α-Al_2O_3 α-Al_2O_3	Sullivan et al., 2004	SR-UV (e)

γ_0^{BET} = 6×10^{-6} ($[O_3]=2\times10^{12}$ cm^{-3})	298		Sah. D.	Chang et al., 2005	SR-UV (e)
γ_0^{BET} = 2×10^{-7} ($[O_3]=10^{14}$ cm^{-3})			Sah. D.		
γ_{ss}^{pd} = $(2.7\pm0.3)\times10^{-6}$	298		kaolinite	Karagulian and Rossi, 2006	Kn-MS (f)
γ_{ss}^{pd} = $(7.8\pm0.7)\times10^{-7}$	298		$CaCO_3$		
γ_{ss}^{BET} = $(3.5\pm0.9)\times10^{-8}$ ($[O_3]=9.8\times10^{14}$ cm^{-3})	298	0	α-Al_2O_3	Mogili et al., 2006	SR-UV/FTIR aerosol chamber (g)
γ_{ss}^{BET} = $(4.5\pm0.9)\times10^{-9}$ ($[O_3]=1.1\times10^{15}$ cm^{-3})		19	α-Al_2O_3		
γ_{ss}^{BET} = $(1.0\pm0.3)\times10^{-7}$ ($[O_3]=6.8\times10^{14}$ cm^{-3}, dry)		0	α-Fe_2O_3		
γ_{ss}^{BET} = $(5.0\pm1.2)\times10^{-8}$ ($[O_3]=1.9\times10^{14}$ cm^{-3})		0	α-Fe_2O_3		
γ_{ss}^{BET} = $(4.4\pm1.1)\times10^{-9}$ ($[O_3]=8.5\times10^{14}$ cm^{-3}, dry)		41	α-Fe_2O_3		
γ_{ss}^{BET} = $(9.0\pm2.3)\times10^{-9}$ ($[O_3]=7.5\times10^{13}$ cm^{-3}, dry)		43	α-Fe_2O_3		
Partitioning coefficients: K_{linC}					
1.6×10^3 cm	296		Sah. D.	Hanisch and Crowley, 2003	Kn-MS (h)

Comments

(a) Observation of O_3 in reaction vessels using optical absorption at 254 nm in the presence of Ar. Typical ozone and Ar pressures were 1.3-13 and 2.6 mbar, respectively. Mechanistic information and the temperature dependence of the decay rate constants were given for quartz, glass and water surfaces.

(b) Bulk powder samples generated by gently heating an aqueous slurry of the powder on the sample support. The ozone concentration was 1.9×10^{11} cm^{-3}. The initial and steady state γ values shown in the table have been calculated using the BET surface area in the linear mass dependent regime.

(c) Bulk powder samples generated by gently heating an aqueous slurry of the powder on the heated sample support. The ozone concentration was varied from 10^{11} cm^{-3} to 10^{12} cm^{-3}. The initial and steady state γ values shown in the table were calculated using the BET surface area in the linear mass dependent regime. The uptake coefficients were independent of the ozone concentration within the range given. A small temperature dependence of γ was observed, leading to an activation energy of 7±4 kJmol^{-1}. The steady state uptake coefficients were reported for an interaction time of 4.5 h.

(d) Powder samples were prepared by dispersing an aqueous or methanol based paste onto the sample holder and evacuating overnight. Some samples were heated to 450 K prior to use. Steady state uptake coefficients were calculated (extrapolated) based on a bi-exponential fit to the observed uptake curves. The tabulated initial and steady state γ values were corrected using a pore diffusion model. The relative O_2 product yield varies from 1.0 to 1.3 ± 0.05 for unheated and heated (450K, 5h under vacuum) samples, respectively. Release of water correlated with the ozone concentration. Passivated samples could be reactivated by evacuation overnight.

(e) Static reaction cell (Pyrex) equipped with detection of O_3 using UV absorption at 254 nm. The dust powder was coated onto the surface by applying a methanol slurry and drying without heating. The BET surface area was 2.2 m^2/g for alumina and 14 m^2/g for Saharan

dust. Decay of O_3 over the first 10 s of exposure were converted to the listed γ_0, γ_0 was constant for O_3 concentrations between 10^{12} and 10^{13} cm^{-3} for alumina and was inversely proportional to the O_3 concentration above 10^{13} cm^{-3} for both alumina and Saharan dust. γ does not change with humidity in the range 0 to 75% rh. A significant degree (over 50 % of initial value) of was observed following storage of the used samples in a container purged with dry and CO_2-free air for a few days. No products were detected.

(f) Steady state and pulsed uptake experiment on powder substrates. γ was obtained using a pore diffusion model for the data on kaolinite and $CaCO_3$. For $CaCO_3$, uptake to a sample of roughened marble resulted in an uptake coefficient of 3.5×10^{-5}, which is a factor 50 higher than the one obtained for the $CaCO_3$ powder sample after pore diffusion correction. For Saharan dust and Arizona test dust, only uptake coefficients referred to the geometric sample surface area are reported. The SD sample showed a factor of 2 decrease in reactivity with O_3 concentration increasing from 3.5×10^{12} to 1.0×10^{13} cm^{-3}. In general, initial uptake coefficients were a factor of 3 to 10 higher than steady state values. The only gas phase product detected was O_2. The O_2 yield per O_3 consumed showed significant variation from 0.0 to 2.0.

(g) Powder samples were evacuated prior to use and then injected into a 0.15 m^3 chamber. The aerosol was not further characterized. The surface to volume ratio of the aerosol used to calculate uptake coefficients was taken from the injected sample mass and the BET surface area of the sample measured separately. O_3 was detected using FTIR or UV absorption. Under dry conditions, for α-Fe_2O_3, the number of O_3 molecules lost divided by the number of available surface sites, was 2 or more, indicating catalytic reactivity. For α-Al_2O_3, less than one O_3 was lost per reactive site. The uptake coefficient decreased gradually with increasing O_3 concentration and decreased by a factor of 50 when relative humidity was increased from dry to 58 %.

(h) Saharan dust samples were deposited on a sample holder in the form of an ethanol paste. The experiment was aimed at determining NO to NO_2 oxidation rates as a function of O_3 concentration. The rates were fitted assuming Langmuir adsorption of both NO and O_3 prior to reaction. The value of K_{LinC} given in the table has been derived from K_{LangC} = 4×10^{-12} cm^3 reported by the authors and an assumed $N_{max} = 4 \times 10^{14}$ cm^{-2}.

Preferred Values

Parameter	Value	T/K
γ	$1500\ [O_3\ (cm^{-3})]^{-0.7}$	298
Reliability		
$\Delta \log(\gamma)$	± 0.5	298

Comments on Preferred Values

Given the different techniques used to obtain kinetic data, the data agree fairly well, when considering the strong dependence of the steady state uptake coefficients on ozone concentration, which has also been discussed in most of the studies cited. The initial uptake coefficients are more difficult to compare as they seem to depend more on the way the samples were exposed, and possibly also on the treatment of the samples prior to the experiment (heating, evacuation). Also the time resolution of the experiments is different, which makes the interpretation of initial uptake coefficients difficult without explicit kinetic modelling of especially the static and aerosol experiments. Probably because of the small steady state reactivities, interpretation of the kinetic data using the BET surface area of the powder samples in the linear mass dependent regime or using pore diffusion theory led to fairly consistent results. We therefore use only uptake coefficients derived from steady state uptake data that are referred to the BET surface area in our evaluation. The earlier study by

Alebic-Juretic et al. (1992) is in qualitative agreement with the studies cited here, but does not directly provide quantitative kinetic data.

Considering the steady state values only, the Saharan dust, kaolinite, Al_2O_3, Fe_2O_3 and $CaCO_3$ agree surprisingly well with each other. We used the available Saharan dust data to obtain a recommendation of the uptake coefficient as a function of ozone concentration in the range of 10^{10} to 10^{13} cm^{-3}, for relative humidity below 5%.

All studies note the potential effects of humidity, which has a significant effect on spectroscopic signatures on alumina observed in DRIFTS experiments (Roscoe and Abbatt, 2005; see below). Sullivan et al. (2004), however, found no humidity dependence in their kinetic experiments using the same type of samples. On the other hand, Mogili et al. (2006) report a significant humidity dependence of the uptake coefficient, which was reduced by a factor of 50 from dry to 60% relative humidity for Fe_2O_3 and a factor of about 10 from dry to 20% relative humidity for Al_2O_3.

Given the consistent dependence of steady state uptake coefficients of the ozone concentration, the rate limiting step in the mechanism of the reaction of ozone with mineral dust seems to be common among the different materials investigated, even in the atmospherically relevant concentration range around 10^{12} cm^{-3}. This mechanism may be represented by the following reactions, which have been consistently proposed in most studies:

$$O_3 + SS \rightarrow SS\text{-}O + O_2 \qquad (1)$$

$$SS\text{-}O + O_3 \rightarrow SS\text{-}O_2 + O_2 \qquad (2)$$

Therein, SS denotes a reactive surface site, which are likely Lewis acid sites as present on alumina or Fe_2O_3 that are susceptible to dissociative adsorption of O_3, a Lewis base. Since desorption of O_3 from a dust surface has never been observed, the idea of a Langmuir-Hinshelwood type reaction as mechanism for (1) to explain the negative O_3 pressure dependence has remained uncertain. Lampimäki et al. (2013) indeed observed reversible changes to the surface potential upon exposure of Fe_2O_3 and TiO_2 to O_3 based on photoelectron spectroscopy experiments. They suggested that charge transfer to O_3 may occur and argued that due to the relatively poor screening ability of the dielectric materials the maximum coverages would remain limited to below the percent level of a monolayer. Such small coverages would remain undetected in desorption mode flow tube experiments. Since Lampimäki et al. did not quantify the surface coverage of these intermediates, we nevertheless do not recommend a value for K_{LinC}. It would still be plausible that complete oxidation of all available SS to SS-O, which is the reactive species towards NO and O_3, explains the saturation behaviour observed by Hanisch and Crowley (2003b).

It is likely that in the experiment by Hanisch and Crowley (2003a) the O_3 loss kinetics was driven by uptake due to reaction (1) at the lower O_3 concentration. An oxidised surface species SS-O is consistent with IR spectroscopic features observed by Roscoe and Abbatt (2006). The formation of the second, peroxy species, by reaction (2) has been suggested based on a study of O_3 decomposition on MnO (Li et al., 1998), but could not be observed by Roscoe and Abbatt (2006), because the IR signature was outside the wavelength region they probed.

Overall, reactions (1) and (2) can explain catalytic loss of ozone whereby up to two O_3 are lost per surface site, along with the formation of O_2 as a product (Mogili et al., 2006; Karagulian et al., 2006). Slow decomposition of $SS\text{-}O_2$ and self reaction of SS-O have been suggested to release reactive SS again, which would establish a catalytic cycle for ozone destruction. The time scale of reactivation observed in the experiment was on the order of a day.

The role of humidity in the reaction mechanism is not clear. On one hand, hydroxylated surface sites seem to be involved in reaction (1) (Hanisch and Crowley, 2003a), while water can be involved in removing oxygen from SS-O as observed by Roscoe and Abbatt (2006), which would also explain the strong humidity dependence observed by Mogili et al. (2006), though at very high O_3 concentrations. Therefore, humidity on one hand can competitively adsorb to reactive sites and therefore reduce the uptake coefficient, while on the other hand, it may lead to reactivation of oxidised surface sites.

In view of the significant uncertainties related to the mechanism (details of reactions (1) and (2), humidity dependence, reactivation processes), we have allowed for a relatively large uncertainty associated with the recommended steady uptake coefficients. We also note that no studies exist on the impact of UV radiation on the uptake coeffient or on reactivation.

References

Alebic-Juretic, A., Cvitas, T., and Klasinc, L.: Ber. Bunsenges. Phys. Chem., 96, 493-495, 1992.

Chang, R. Y. W., Sullivan, R. C., and Abbatt, J. P. D.: 32, art. No. L14815, 2005.

Hanisch, F., and Crowley, J. N.: Phys. Chem. Chem. Phys., 5, 883-887, 2003b.

Hanisch, F., and Crowley, J. N.: Atmos. Chem. Phys., 3, 119-130, 2003a.

Ill'in, S. D., Selikhanovich, V. V., Gershenzon, Y. M., and Rozenshtein, V. B.: Sov. J. Chem. Phys., 8, 1858-1880, 1991.

Karagulian, F., and Rossi, M. J.: Int. J. Chem. Kin., 38, 407-419, 2006.

Lampimäki, M., Zelenay, V., Křepelová, A., Liu, Z., Chang, R., Bluhm, H., and Ammann, M.: ChemPhysChem, 14, 2419-2425, 2013.

Li, W., Gibbs, G. V., and Oyama, S. T.:, J. Am. Chem. Soc., 120, 9041-9046, 1998.

Michel, A. E., Usher, C. R., and Grassian, V. H.: Geophys. Res. Lett., 29, art. no.-1665, 2002.

Michel, A. E., Usher, C. R., and Grassian, V. H.: Atmos. Environ., 37, 3201-3211, 2003.

Mogili, P. K., Kleiber, P. D., Young, M. A., and Grassian, V. H.: J. Phys. Chem. A, 110, 13799-13807, 2006.

Roscoe, J. M., and Abbatt, J. P. D.: J. Phys. Chem. A, 109, 9028-9034, 2005.

Sullivan, R. C., Thornberry, T., and Abbatt, J. P. D.: Atmos. Chem. Phys., 4, 1301-1310, 2004.

Usher, C. R., Michel, A. E., Stec, D., and Grassian, V. H.: Atmos. Environ., 37, 5337-5347, 2003.

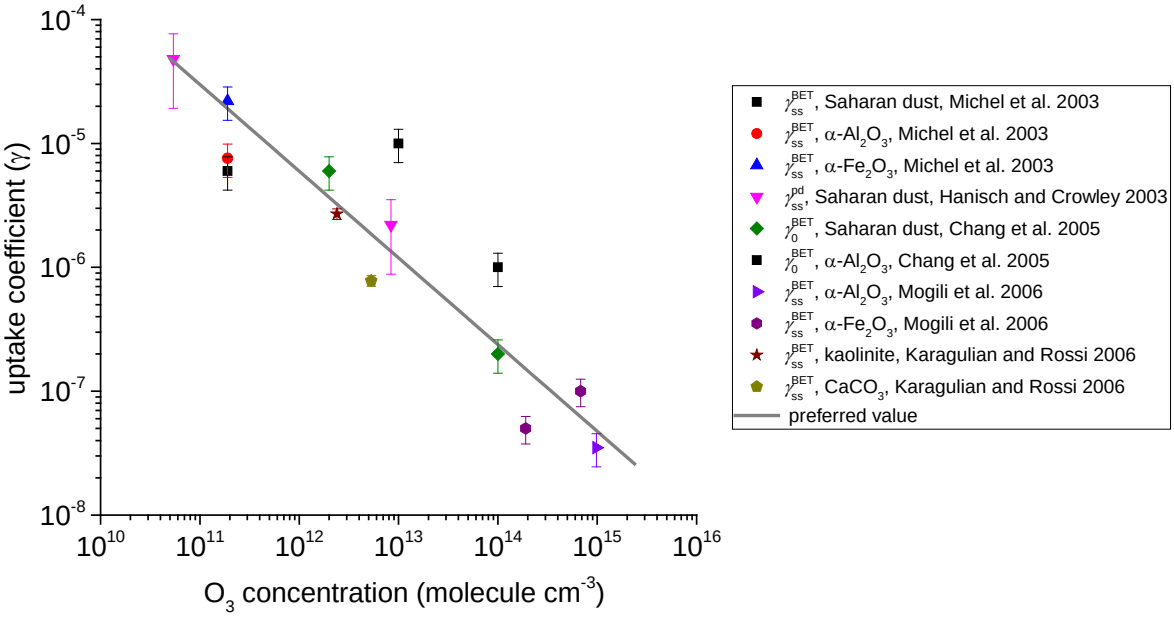

Figure 1: Steady state uptake coefficients reported for mineral dust (symbols) along with the preferred parameterization (line)